Optical Frequency Modulation Links: Theory and Experiments

Bo Cai and Alwyn J. Seeds, *Fellow, IEEE*

***Abstract*—In this paper, the first theoretical analysis and experimental realization of an optical frequency modulation coherent detection (FMCD) link working at microwave frequencies is reported. Advantages over conventional optical intensity modulation direct detection (IMDD) links in terms of reduced effects of fiber nonlinearity, facilitation of multichannel operation, and bandwidth/signal-to-noise ratio (SNR) tradeoffs are identified. A detailed theoretical analysis of the SNR of FMCD links is carried out and compared to that for IMDD links. In the experimental FMCD link, a novel source laser tuning technique, based on the quantum confined Stark effect, is used. The experimental results are presented and compared with the predictions of the theoretical analysis.**

***Index Terms*— Coherent optical communication, microwave photonics, optical fiber links, quantum well, semiconductor laser.**

I. Introduction

OPTICAL fiber provides a wide optical transmission bandwidth for analog optical links. Currently, most optical analog transmission systems use optical intensity modulation direct detection (IMDD) of the modulated optical signal in a depletion photo-detector [1], [2] and only utilize a fraction of this available bandwidth. In such a system, although the link dynamic range can be improved significantly by high power sources and optical amplifiers, as shown later in this paper, it is limited ultimately by shot noise and transmission medium (fiber) nonlinearity [3], [4].

An alternative approach, which can overcome these limitations, is to use optical frequency modulation coherent detection (FMCD) of the transmitter [5]. In such an approach, the signal is carried by the frequency rather than the intensity of the transmitter output. Apart from high signal-to-noise ratio (SNR), this approach also has advantages of constant transmission power, high detection sensitivity, and multichannel transmission capability.

An FMCD link consists of transmitter, receiver, and transmission medium, usually single-mode optical fiber. A frequency tuneable light source is used in the transmitter to convert an incoming electronic signal to an optical FM signal. At the receiver, the signal is down-converted using an optical local oscillator and detected by a depletion photo-detector. Demodulation is then carried out by an electronic frequency discriminator.

In this paper, optical FM analog links are analyzed and the first experimental demonstration is reported, including the use of a novel tuneable laser as the transmitter. In Section II, the performance of an FMCD link is analyzed in terms of its signal-to-noise ratio. Comparison is made with the SNR limits of IMDD links to demonstrate the advantages of the FMCD link. In Section III, the FMCD link experiment is detailed and link bandwidth and SNR results are presented. Conclusions are drawn in Section IV.

II. Basic Concept and Advantages of an Optical FMCD Link

An optical FMCD system is a direct emulation of RF FM broadcast and communications systems in the optical domain and uses the same basic concepts. In an optical link, the laser output provides a carrier of very high frequency (200–400 THz). As with RF carriers, there are two independent characteristics, amplitude and phase or frequency, which can be modulated with the signal to be transmitted. In optical FM (OFM) the carrier frequency deviates from its central frequency proportionately to the amplitude of the signal to be transmitted. Both random and impulse noise can be reduced by using a wide passband receiver containing an amplitude limiter. Therefore, for received carrier to noise ratios much greater than unity, FM systems can provide improved SNR relative to amplitude modulated systems.

The OFM system has three main features which distinguish it from its RF equivalent. First, the optical carrier frequency is very high relative to the bandwidth of the signal to be transmitted. As a result, a large frequency deviation relative to the signal bandwidth can easily be achieved with good linearity. On the other hand, a small relative carrier frequency drift will be significant compared with the signal bandwidth. Second, because no photo-detector has a bandwidth matching the optical carrier frequency, either demodulation in the optical domain or down conversion of the received signal from optical frequency to a much lower intermediate frequency is needed. Third, due to the high optical carrier frequency, the laser generates far more phase/frequency noise than an RF oscillator. This noise has to be considered in an optical FMCD link and, in fact, can be the major limiting factor on the signal-to-noise ratio.

The basic advantages of an FM system are well documented [6], [7]. The work reported here concentrates on the SNR

Manuscript received April 15, 1996; revised December 24, 1996. This work was supported by the U.K. Department of Trade and Industry/Science and Engineering Research Council LINK Opto-electronic Systems Program through the Wideband Optical Radio Frequency Networks (WORFNET) Project.

The authors are with the Department of Electronic and Electrical Engineering, University College London, London WC1E 7JE U.K.

Publisher Item Identifier S 0018-9480(97)02529-5.

performance of the FMCD link and the performance with that of the contrasts' well-established IMDD link.

A. SNR Limits of IMDD Links

In an IMDD system, as shown in Fig. 1, the analog signal to be transmitted can be represented by $m(t)$. The optical power at the detector is

$$P_o = P_u[1 + \gamma m(t)] \tag{1}$$

where P_u is the mean received optical power and γ is the modulation sensitivity $(\gamma m(t) > -1)$.

The mean squared signal current at the detector output is

$$\langle I_s^2 \rangle = (RP_u\gamma)^2 \langle m^2(t) \rangle \tag{2}$$

where R is the photodiode responsivity.

Noise arises from the transmitter, any optical amplifiers used, and the photodetector. Fundamentally the noise is limited by the quantum nature of photon-matter interaction [8]. Taking into account the thermal noise of the electric circuit and the effective signal bandwidth B, can be derived the current variance for the whole link as

$$\begin{aligned}\sigma_I^2 =& B[(RP_u)^2 RIN + 2qRP_u + 2P_nP_uR^2 \\ &+ (2\Delta f_{\text{op}} - B)P_n^2R^2 + 4kT/R_l]\end{aligned} \tag{3}$$

where RIN represents the excess intensity noise due to noncoherent behavior of the transmitter, q is the electronic charge, $P_n = 2hfG(l)\int_0^l g(z)/G(z)\,dz$ is the optical amplifier spontaneous emission (ASE) noise, l is the total link length, $g(z)$ is the gain coefficient at position z, $G(z) = \exp\{\int_0^z [g(z') - \alpha(z')]\,dz\}$ is the total link gain/loss at position z, k is Boltzmann's constant, T is the absolute temperature, R_l is the receiver load resistance, and Δf_{op} is the link optical filter bandwidth. Electrical pre-amplifier noise is neglected in the derivation of the above equation.

The terms in (3) correspond to the amplified transmitter RIN, detector shot noise, ASE-signal beat noise, ASE-ASE beat noise and thermal noise, respectively. The SNR of the link can be written as (see (4) at the bottom of the page). The SNR can be improved by increasing the power received at the detector. The detector received power P_u is, however, limited by stimulated Brillouin scattering (SBS) in the transmission fiber. For the worst case of a source laser of narrow linewidth relative to the SBS gain bandwidth (30 MHz at 1.55 μm), the SBS threshold for P_u in nonpolarization preserving single-mode fiber is given by [9]

$$P_{\text{SBS}} = \frac{21\pi D_e^2 G(l)}{2g_B \int_0^l G(z)\,dz} \tag{5}$$

where D_e is the effective fiber core diameter and g_B is the SBS gain factor.

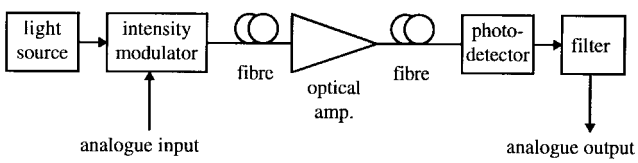

Fig. 1. IMDD transmission system.

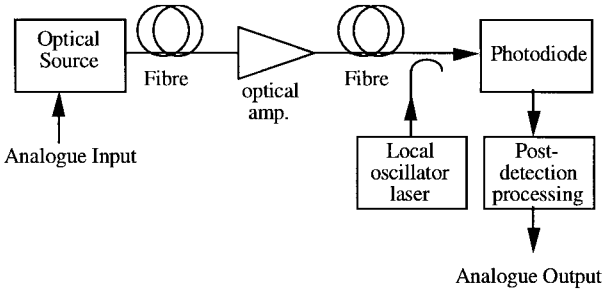

Fig. 2. Optical FMCD link.

Without optical amplifiers in the link, $g(z) = 0$. The SNR for such a passive IMDD fiber link with 100% modulation and $\langle m^2(t) \rangle = 0.5$ is plotted in Fig. 3. The results show a rapid SNR degradation with link length.

By inserting optical amplifiers in the link, the received optical power at the photo-detector will increase and so will the shot noise limited SNR. However, the optical amplifiers will also introduce ASE noise to the link. In an optimized transparent link, the signal is amplified by low gain, closely spaced optical amplifiers. In this ideal case, the optical gain can be considered distributed along the whole link exactly compensating the loss as it occurs. In such a case, if the fiber loss coefficient α is constant, then $g(z) = \alpha$, $G(z) = 1$, $P_n = 2hf\alpha l$. The SNR against link length for this case is plotted in Fig. 3. The results show that even in the ideally amplified case, the SNR of IMDD links is limited. For short links without optical amplifiers, the SNR is likely to be limited by RIN and shot noise and for long links with optical amplifiers, the SNR is likely to be limited by ASE. In reality, the SNR will be further reduced by other noise sources.

B. SNR Limits of FMCD Links

In an FMCD link, as shown in Fig. 2, the signal electric field at the photodiode is

$$E_s = \hat{E}_s \exp\left\{ j\left[\omega_s t + 2\pi\Delta f \int_0^t m(\tau)\,d\tau + \varphi_s(t)\right]\right\}$$

where $\hat{E}_s$ and ω_s are the amplitude and frequency of the field, Δf is the maximum frequency deviation, $\varphi_s(t)$ is the random initial phase and $m(\tau)$ is the normalized signal varying from -1 to 1. The local oscillator electric field is

$$E_{\text{LO}} = \hat{E}_{\text{LO}} \exp\{j[\omega_{\text{LO}} t + \varphi_{\text{LO}}(t)]\}$$

$$\text{SNR} = \frac{(RP_u\gamma)^2 \langle m(t) \rangle^2}{B[(RP_u)^2 RIN + 2qRP_u + 2P_nP_uR^2 + (2\Delta f_{\text{op}} - B)P_n^2R^2 + 4kT/R_l]} \tag{4}$$

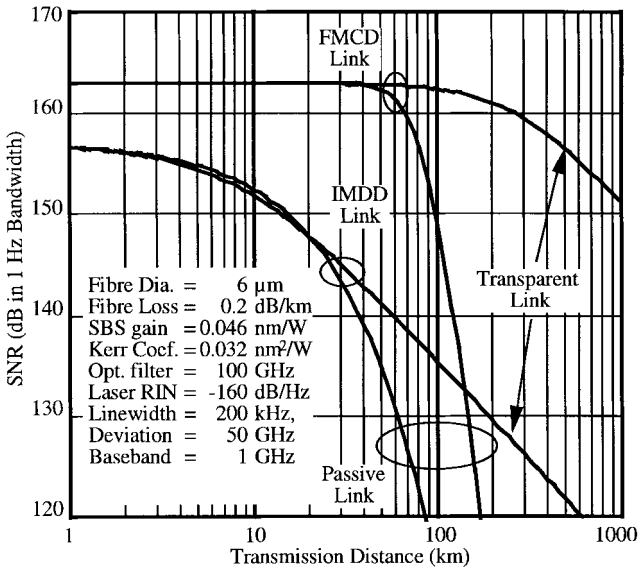

Fig. 3. SNR characteristics of IMDD and FMCD links.

with $\omega_{\rm LO}$ being the local oscillator frequency and $\varphi_{\rm LO}$ the local oscillator phase. Assuming E_s and $E_{\rm LO}$ are polarization matched at the photodiode surface and taking into account that $\hat{E}_s^2 \propto P_u$ and $\hat{E}_{\rm LO}^2 \propto P_{\rm LO}$, the output current of the photodetector can be expressed as

$$I(t) = I_0 + I_s \cos\left[\omega_{\rm IF} t + 2\pi\Delta f \int_0^t m(\tau)\,d\tau + \varphi_s - \varphi_{\rm LO}\right]$$

where $I_0 = R(P_{\rm LO} + P_u)$, $I_s = 2R\sqrt{P_{\rm LO}P_u}$ and $\omega_{\rm IF} = \omega_s - \omega_{\rm LO}$. At the FM discriminator output, the mean squared signal current is

$$\langle i_s^2\rangle = \Gamma_{\rm FM}^2 \Delta f^2 \langle m^2(t)\rangle \tag{6}$$

where $\Gamma_{\rm FM}$ is the FM detector gain.

When the local oscillator output power $P_{\rm LO}$ is significantly higher than received signal power P_u the major noise current is contributed by an additive intensity noise related to I_0 and a phase noise φ_n.

The additive noise can be divided into quadrature and in-phase components. The influence of quadrature components on an FM system is well documented [10]. At the FM detector output, the current variance due to quadrature components $\sigma_{\rm qu}^2$ is:

$$\sigma_{\rm qu}^2 = \frac{(B\Gamma_{\rm FM})^2}{3I_s^2}[I_0^2 RIN + 2qI_0 + 2P_n R I_0 + (2\Delta f_{\rm op} - B)P_n^2 R^2 + 4kT/R_l]B. \tag{7}$$

Compared with the photodetector output, the FM detecting and RF filtering processes improve SNR by a factor of $3(\Delta f/B)^3$. For a typical $\Delta f/B$ ratio of 10, a SNR improvement of 35 dB can be achieved.

The in-phase components cause link transmission optical power fluctuation. Through the Kerr effect in the transmission fiber, such fluctuation will generate phase noise at the link output [11], [12]. At the FM discriminator output, the current variance due to the in-phase components $\sigma_{\rm in}^2$ can be linked to optical intensity noise by

$$\frac{d\sigma_{\rm in}^2}{dz} = \frac{2hfB}{3}[B\Gamma_{\rm FM}K_G(z)]^2 \left[\frac{P_u G(z)}{G(l)} + \frac{2\Delta f_{\rm op} - B}{2}P_n(z)\right] g(z) \tag{8}$$

and the boundary conditions determined by transmitter noise at the fiber input

$$\sigma_{\rm in}^2(0) = \frac{B}{3}\left[\frac{B\Gamma_{\rm FM}K_G(0)P_u}{G(l)}\right]^2 \left[RIN + \frac{2hfG(l)}{P_u}\right] \tag{9}$$

where $K_G(z) = \int_z^l G(z')\kappa_2(z')\,dz'$, κ_2 is the transmission medium nonlinear coefficient and for fiber $\kappa_2 = 8n_2/\lambda D_e^2$, n_2 is the Kerr coefficient. Equation (8) characterizes the influence of ASE noise along the transmission line and (9) that of the transmitter at the input of the link.

The laser phase noise passes through the FM discriminator directly and causes noise at the output. The current variance $\sigma_{\rm ph}^2$ is

$$\sigma_{\rm ph}^2 = \frac{\Gamma_{\rm FM}^2}{2\pi}\int_{-\infty}^{\infty} |H(f)|^2 S_f(f)\,df \tag{10}$$

where $H(f)$ is the transfer function of the link, $S_f(f)$ the sum of transmitter and LO laser frequency noise spectral density. Assuming that $\langle m^2(t)\rangle = 0.5$, that the link transmission bandwidth is rectangular ($|H(f)|^2 = 1$ for $f \subset [-B, B]$, $|H(f)|^2 = 0$ otherwise) and the frequency noise is white, then $S_f = 2\pi\delta f$ and (10) reduces to

$$\sigma_{\rm ph}^2 = \Gamma_{\rm FM}^2 B\delta f/\pi \tag{11}$$

where δf is the sum of transmitter and local oscillator (LO) laser spectral linewidth.

Combining (6)–(11) the SNR of an optical FMCD link can be expressed as

$$\text{SNR} = \frac{\Gamma_{\rm FM}^2 \Delta f^2 \langle m^2(t)\rangle}{\sigma_{\rm qu}^2 + \sigma_{\rm in}^2 + \sigma_{\rm ph}^2}.$$

Both passive and ideally amplified link results for typical operating parameters are calculated and plotted in Fig. 3.

Fig. 3 shows that the SNR of an FMCD system is primarily determined by the transmitter and LO laser linewidth δf and the maximum frequency deviation Δf which is, in turn, limited by photodiode bandwidth. For long links, the SNR can be improved by bandwidth-SNR tradeoff. Compared with IMDD, FMCD links can show significant advantages in SNR performance.

III. Experiments

An FMCD link has been constructed, as shown in Fig. 4, to demonstrate the principles described above. The input signal modulates the optical frequency of the tuneable optical source and the resulting signal passes through the link to the receiver. An LO laser is offset from the source center frequency by the intermediate frequency (IF), which is made greater than the peak source frequency deviation. Balanced photo detection is preferred to minimize the contribution from LO laser intensity

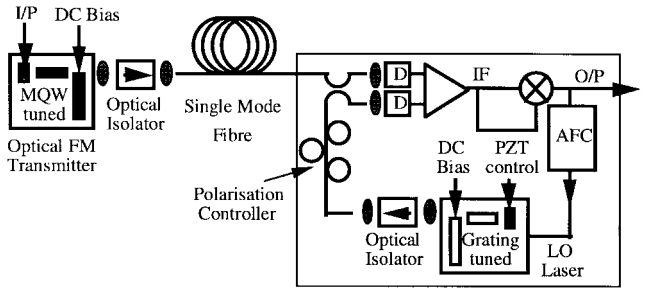

Fig. 4. Experimental optical FMCD link.

noise. The effect of intensity noise is further reduced by using a limiting IF amplifier. Signal recovery is by delay line microwave frequency discriminator, which also drives the LO laser frequency control circuit to compensate for system drift.

One of the biggest challenges in implementing such a system is to build a suitable tuneable optical source as the transmitter laser. The continuous tuning range of the source must be reasonably large in order to take full advantage of the available bandwidth of the photo-detector and the linewidth of the source must be narrow enough, relative to its tuning range, to achieve large signal-to-noise ratio. Furthermore, the bandwidth of the link will depend on the FM frequency response of the source; a wide and uniform FM frequency response is required to realize wide link bandwidth. To fulfill these crucial demands, a novel source laser tuning technique based on the quantum confined Stark effect (QCSE) in quantum-well materials is used in a multiple quantum-well (MQW) tuned external cavity laser [13]. In the MQW-tuned external cavity laser, a part of the laser cavity is formed by the MQW material. Due to QCSE, the refractive index of the MQW material can be modulated at very high speed by an electric field applied across it. This causes modulation of the optical length of the laser cavity and, therefore, of the emitted optical frequency.

Fig. 5 shows the MQW-tuned external cavity laser. A 300-μm long GaAs/AlGaAs channelled substrate planar (CSP) laser diode (Hitachi HLP 1400) was used as the laser gain section. One of the laser diode facets was antireflection coated with a single quarter wavelength SiO layer to reduce the Q factor of the laser diode internal cavity modes. The output from this facet was coupled into the tuning element through a graded refractive index (GRIN) lens of 0.29 pitch to form an external cavity laser of optical resonator length 15 mm. The conjugation between the laser diode facet and tuning element window enables the use of a small window area tuning element. The laser diode and MQW tuning element were temperature controlled independently and their relative positions were aligned with piezoelectric translator (PZT) micropositioners.

The tuning element was a PIN-type reflection phase modulator consisting of three sections: 1) the P-doped Bragg reflector section used 12 pairs of 692 Å AlAs/594 Å $Al_{0.2}Ga_{0.8}As$ layers to give a 20-nm wide reflection band centered on 828 nm with power reflection greater than 95%; 2) the intrinsic MQW section comprised 75 pairs of 60-Å $Al_{0.3}Ga_{0.7}As$ barriers and 52 Å GaAs wells, giving a maximum refractive

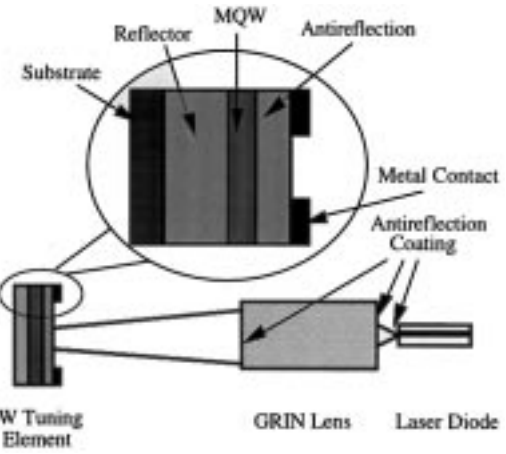

Fig. 5. MQW tuned external cavity laser.

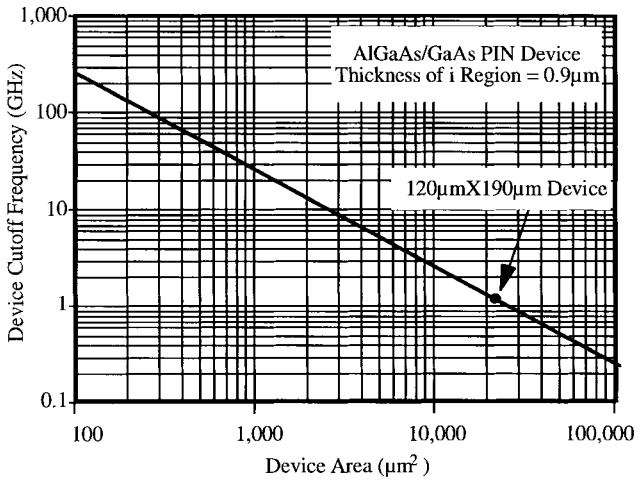

Fig. 6. Cutoff frequencies for different tuning element areas.

index change of 3% at a wavelength of 828 nm under an applied electric field strength of 55kV/cm; and 3) the N-doped antireflection section used 3-1/2 pairs of 692 Å AlAs/587 Å $Al_{0.17}Ga_{0.83}As$ layers giving a 15-nm-wide antireflection band centered on 828 nm with residual power reflection less than 1%. The performance evaluation and wavelength calibration of the three sections were carried out on three separately grown test wafers. The Ga concentration level in both Bragg reflector and antireflection sections was carefully chosen to give adequate reflection and antireflection bandwidth without significant increase of absorption. The whole structure was grown on a semi-insulating substrate using atmospheric pressure metalorganic vapor phase epitaxy (MOVPE) and the conventional reagents of trimethylgallium, trimethylaluminum, and arsine.

Electrically, such a PIN structure is comparable to a parallel plate capacitor. Its capacitance, and therefore the cutoff frequency is directly affected by the device area. For the wafer structure used, the calculated -3 dB cutoff frequencies for different device areas are plotted in Fig. 6. In order to achieve high-frequency operation, Mesa-type tuning elements of area 120 μm$\times$ 190 μm with 50 μm$\times$ 50 μm windows, as shown in Fig. 7, were fabricated from this material using conventional processing techniques.

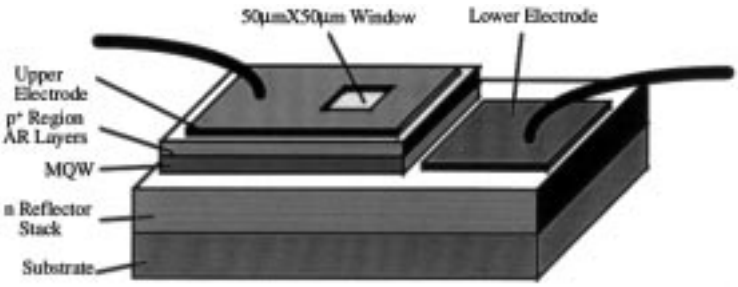

Fig. 7. MQW tuning element structure.

With 5 V reverse bias change on the MQW PIN tuning element, a continuous tuning range of 2.3 GHz was achieved. Harmonic distortion products were better than 30 dB below the signal and unwanted intensity modulation less than 0.3 dB for a peak deviation of 1.5 GHz. The tuning range could be increased by either reducing the external cavity length or increasing the thickness of the MQW section in the tuning element. As the tuning range achieved was sufficiently large to demonstrate the principles of the FMCD link, no effort was made to increase it further.

The laser spectral linewidth was measured to be less than 100 kHz, limited by the resolution of the self homodyne system used.

The FM response of the laser was measured independently by two methods, an adjustable Hi–Bi fiber optical frequency discriminator and a high resolution scanning Fabry–Perot interferometer.

An FM response uniform within ± 1.6 dB from 20 kHz to 1.3 GHz was achieved [13]. The flatness at low frequency clearly shows the absence of the thermal effects which are normally dominant for forward biased, current tuned lasers. The higher frequency limit is due to the capacitance of the MQW tuning element used.

The uniform FM response results confirm the superiority of the tuning mechanism based on QCSE in MQW material over conventional current tuning. The residual IM was about 4% for a peak frequency deviation of 2 GHz.

The LO laser was realized using a grating-tuned external cavity configuration. The output from the SiO antireflection coated facet of the gain section (Hitachi HLP 1400) was collimated by a diffraction limited 10×0.17 numerical aperature (NA) microscope objective lens and diffracted by an 8 mm $\times$ 8 mm, 1200 pair lines/mm, blazed grating, mounted on a miniature PZT mirror mount, forming a 15-mm length external cavity. Both the lens position and grating angles were independently controlled using PZT devices. A full width at half maximum (FWHM) linewidth of less than 100 kHz and sidemode suppression of greater than 30 dB at an output power level of 4 mW were measured using the delayed self-homodyne technique and an optical spectrum analyzer, respectively. By rotating the grating, a large discrete tuning range of over 5 nm which is desired for channel selection potential was achieved.

The optical outputs from both the transmitter and LO laser were combined in a 3-dB fiber coupler and illuminated the photodiode active area. The polarization state of the output from the LO laser was adjusted to match that of the transmitter laser with a fiber polarization controller. In this demonstration set-up, only a single detector was used to simplify the front-end design. The photodiode, mounted on an SMA connector, was an indium tin oxide (ITO) Schottky GaAs diode with a 3-dB cutoff frequency of 18 GHz and responsivity of 0.4 A/W (quantum efficiency of 60%). The transmitter and LO laser power at the detector were approximately 6 and 200 μW, respectively.

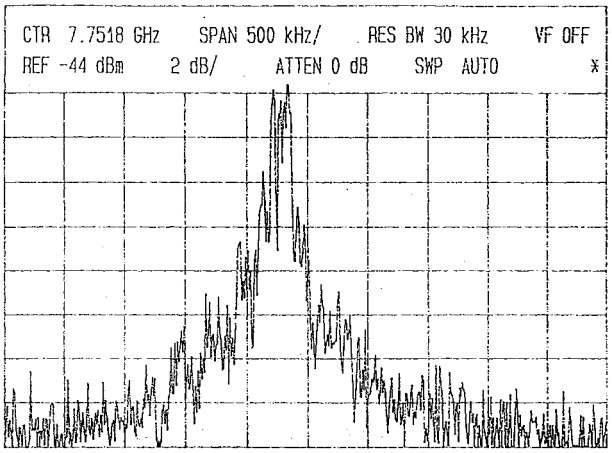

Fig. 8. Detected heterodyne spectrum.

Although the laser emission wavelengths were aligned by grating tuning of the LO laser, further alignment was needed to obtain the desired intermediate frequency f_{if}. This alignment was realized by adjusting the temperature, bias level, and external cavity length of both lasers. The heterodyne signal at 8 GHz is shown in Fig. 8. The linewidth of the beat signal is about 200 kHz, slightly wider than expected due to relative frequency shift during the scanning period of the microwave spectrum analyzer. With a total linewidth of 200 kHz and maximum frequency deviation of over 2 GHz, the achievable SNR limited by laser frequency noise is greater than 130 dB $\cdot$ Hz.

The heterodyne signal in the microwave domain enables a detailed evaluation of laser noise due to the high spectral resolution available. The noise was in the form of both fast jitter and slow drift within a few MHz range. The structure of the noise indicates that the noise was caused by very weak external feedback and instability of both external cavity lasers due to the coupling of residual reflections to the laser diodes. The noise can be reduced by a better experimental environment or better thermal and mechanical isolation from the environment. The slow drift of frequency can be controlled by an automatic frequency control (AFC) loop.

The baseband signal was recovered using a microwave delay line frequency discriminator. The circuit used is shown in Fig. 9. Post-detector amplification was provided by a two-stage IF amplifier. The amplified signal was split by a 90° 3-dB hybrid coupler. The mixer reflections were reduced by circulators in both paths. The phase shifter in one of the paths provided an adjustable delay of 0 to 250 ps. The signals from the two paths were compared in a diode ring double-balanced mixer. Designed as a first-order discriminator, the delay time τ_d and

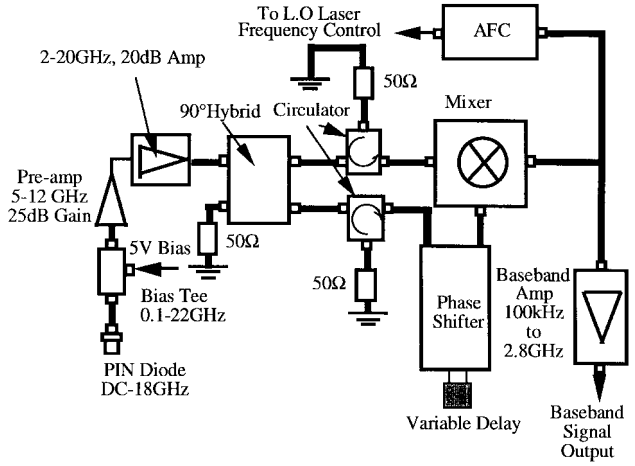

Fig. 9. Signal detection and demodulation circuit.

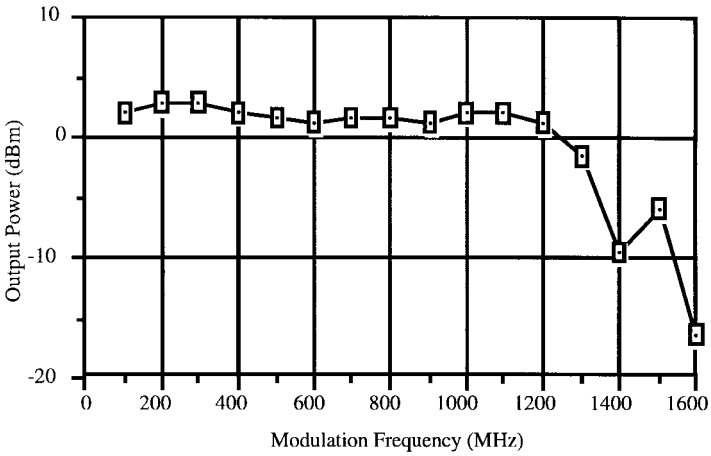

Fig. 10. Link frequency response.

intermediate frequency f_{IF} have the relationship

$$\tau_d \cdot f_{\mathrm{IF}} = 1/2$$

for $f_{\mathrm{IF}} = 8$ GHz, $\tau_d = 62.5$ ps. The demodulated signal from the mixer output was amplified by a baseband amplifier.

Replacing the photodiode with a microwave signal generator and the baseband amplifier with a voltage/current recorder, the static discriminator response was characterized and ripples were observed in the discriminator conversion curve. This is due to imperfect matching at the double-balanced mixer ports and limited the obtainable link linearity.

The flatness of the link transmission frequency response was measured by monitoring the link output signal at different input signal frequencies for a given input signal power. In this case, an input power of 15 dB was used to modulate the MQW tuning element in the transmitter laser. The measurements were taken at 100-MHz frequency intervals. The measured results are plotted in Fig. 10. The results show that with this novel tuning technique an uniform link transmission response to 1.3 GHz (-3 dB) was achieved and the earlier optical spectrum measurements of the transmitter laser FM response were confirmed. The main limitation on the high-frequency response is caused by tuning element depletion capacitance, and the technique could be extended to millimeter-wave frequencies with low parasitic capacitance tuning elements.

The maximum signal-to-noise ratio was estimated by measuring the link output signal and noise power at a given frequency with input signal power set at the 1-dB compression point. The measurement was carried out at 500 MHz, which is the center of the designed bandwidth. For a received optical signal power of 6 μW at the photodetector, a midband output SNR of 120 dB $\cdot$ Hz was achieved after correcting for the spectrum analyzer log amplifier response. This represents an improvement of some 20 dB over an intensity modulated link with the same received power [14]. The characteristic triangular shape of the link noise spectrum confirmed the theoretically predicted SNR-bandwidth tradeoff ability of the link. However, the measured SNR is lower than the value of 130 dB $\cdot$ Hz predicted from laser linewidth limited SNR because the LO laser power is not sufficient to achieve shot noise limited carrier-to-noise ratio (CNR) and full limiter action at the mixer for FM SNR improvement. The link nonlinearity due to imperfection in the microwave frequency discriminator construction also contributes to the reduction of the SNR.

The nonlinearity of the link was observed by harmonic distortion measurement and was mainly contributed by the microwave frequency discriminator. With very irregularly shaped ripples in the FM conversion curve, the conventional means used to quantify the nonlinearity of a link can not be applied. An indirect assessment on the linearity of the link without the influence of the ripples was made using measured transmitter linearity and a perfect sinusoidal FM conversion curve for the frequency discriminator. The results show that the maximum harmonic peaks are more than 30 dB below the signal at the 1-dB compression drive level of 18 dB and high linearity should, therefore, be possible with improved frequency discriminator construction.

IV. Conclusions

An analog optical FMCD link working at microwave frequencies has been analyzed and demonstrated in this paper for the first time. In the experiments, a bandwidth of 1.3 GHz and a SNR of 120 dB$\cdot$Hz were achieved for a received optical power of 6 μW. With the external cavity type source and LO lasers used, the bandwidth can be expanded to 6 GHz by reducing the tuning element depletion capacitance. The SNR obtained was limited by photodiode power handling/LO laser-power capabilities. The SNR can be improved to 130 dB$\cdot$Hz by using a high-power handling photodiode and increasing the LO laser launch power to above -3 dB. Combining the QCSE tuning technique used in these experiments and narrow linewidth laser techniques developed by [15], an optical FMCD link with 50-GHz bandwidth and 160 dB $\cdot$ Hz should be achievable.

Acknowledgment

The authors would like to thank their industrial and academic colleagues for their contributions to this paper. The authors would also like to thank Dr. J. S. Roberts at the EPSRC

III-V Centre, Sheffield University, for growing MQW epitaxial layer required for the source laser tuning elements.

REFERENCES

[1] C. H. Cox, G. E. Betts, and L. M. Johnson, "An analytic and experimental comparison of direct and external modulation in analog fiber-optic links," *IEEE Trans. Microwave Theory Tech.*, vol. 38, pp. 501–509, May 1990.
[2] W. E. Stephens and T. R. Joseph, "System characteristics of direct modulated and externally modulated RF Fiber optic link," *J. Lightwave Technol.*, vol. 5, pp. 380–387, Mar. 1987.
[3] E. P. Ippen and R. H. Stolen, "Stimulated brillouin scattering in optical fibers," *Appl. Phys. Lett.*, vol. 21, p. 539–540, Dec. 1972.
[4] A. R. Chraplavy, "Non-linear effect in optical fibers," in *Topics in Lightwave Transmission Systems*, T. Li, Ed. San Diego, CA: Academic, pp. 267–295, 1991.
[5] B. Cai and A. J. Seeds, "Optical frequency modulation link for microwave signal transmission," in *IEEE Microwave Theory Techniques '94, Dig.*, San Diego, CA, 1994, pp. 163–166.
[6] V. D. Pol, "The fundamental principles of frequency modulation," *Proc. Inst. Elect. Eng.*, vol. 93, pt. III, pp. 153, 1946.
[7] T. Kimura, "Coherent optical fiber transmission," *J. Lightwave Technol.*, vol. 5, pp. 414–428, Apr. 1987.
[8] E. Desurire, "Erbium-doped fiber amplifiers: Principles and applications," New York: Wiley, 1994.
[9] R. G. Smith, "Optical power handling capacity of low loss optical fibers as determined by stimulated raman and brillouin scattering," *Appl. Opt.*, vol. 11, pp. 2489–2494, Nov. 1972.
[10] J. Fagot and P. Magne, *Frequency Modulation Theory: Application to Microwave Links*, New York: Pergamon, 1961.
[11] J. P. Gordon and L. F. Mollenauer, "Phase noise in photonic communications systems using linear amplifiers," *Opt. Lett.*, vol. 15, pp. 1351–1353, Dec. 1990.
[12] S. Ryu, "Signal linewidth broadening due to fiber nonlinearities in long-haul coherent optical fiber communication systems," *Electron. Lett.*, vol. 27, pp. 1527–1529, Aug. 1991.
[13] B. Cai, A. J. Seeds and J. Roberts, "MQW-tuned semiconductor laser with uniform frequency response," *IEEE Photon. Technol. Lett.*, vol. 6, pp. 496–498, Apr. 1994.
[14] A. J. Seeds, "Microwave optoelectronics," *Opt. Quantum Electron.*, vol. 25, pp. 219–229, Apr. 1993.
[15] M. Okai, T. Tsuchiya, K. Uomi, N. Chinone, and T. Harada, "Corrugation-pitch-modulated MQW-DFB laser with narrow spectral linewidth," *IEEE Photon. Technol. Lett.*, vol. 2, p. 529–530, Aug. 1990.

Bo Cai received the B.Eng. and M.Eng. degrees from Xi'an Institute of Technology, Institute of Optics and Electronics, Chinese Academy of Sciences in 1982 and 1985, respectively and the Ph.D. degree from University College London, U.K., in 1991, all in optical engineering and optoelectronics.

Since 1991, he has been with University College London working on fast tuneable lasers, wideband optical links and other aspects of high-speed optical transmission systems. He is currently engaged in research on dense wavelength division multiplex optical communication systems.

Alwyn J. Seeds (M'81–SM'92–F'97) received the B.Sc. degree in electronics and the Ph.D. degree in electronic engineering from the University of London, U.K., in 1976 and 1980, respectively.

From 1980 to 1983 he was a Staff Member at Lincoln Laboratory, Massachusetts Institute of Technology (MIT), where he worked on monolithic millimeter-wave integrated circuits for use in phased-array radar. In 1983, he was appointed Lecturer in Telecommunications at Queen Mary College, University of London, U.K. In 1986 he moved to University College London, U.K., where he is currently Professor of Opto-electronics and leader of the Microwave Opto-electronics Group. He is the author of over 100 papers on microwave and opto-electronic devices and their systems applications and presenter of the video "Microwave Opto-electronics" in the IEEE Emerging Technologies series. His current research interests include microwave bandwidth tunable lasers, optical control of microwave devices, mode-locked lasers, optical phase-locked loops, optical frequency synthesis, dense WDM networks, optical soliton transmission, and the application of optical techniques to microwave systems.